of k_2 and the negative activation energy that they report (−1.4 kcal mol^{-1}).

Summary

This investigation yielded rate constants for the metathesis reaction of *tert*-butyl radical with DBr at 295 and 384 K. After correction for the primary isotope effect, these are a factor of 50 or 11 smaller than obtained by Russell et al.[1] The reaction has a positive activation energy rather than the negative value reported in this same reference.

In combination with the measurements of the reverse reaction of Russell et al.,[1] one obtains

$$\Delta H_f°_{298}(t\text{-}C_4H_9) = 9.2 \pm 0.5 \text{ kcal mol}^{-1}$$

in agreement with previous studies[3,4] of the corresponding DI reaction that has also been remeasured in this study. No evidence for a complex mechanism involving a bound intermediate, as suggested in ref 1 has been found.

Special effort has been made to assess the possible interference of wall contributions and to find an appropriate range of experimental conditions.

Acknowledgment. W.M.-M. thanks the Deutsche Forschungsgemeinschaft for a fellowship and D.M.G.'s time was partially supported by DOE Basic Energy Sciences under Contract No. DE-FG03-86ER13571. Conversations with David Gutman have been friendly and stimulating.

Catalysis of the Enolization of Oxaloacetic Acid by Primary and Secondary Amines via a Carbinolamine Intermediate

Paula Yurkanis Bruice

Contribution from the Department of Chemistry, University of California at Santa Barbara, Santa Barbara, California 93106. *Received August 5, 1987*

Abstract: The reaction of oxaloacetic acid has been investigated with six primary and six secondary amines. The amines were found to catalyze keto–enol interconversion in a rapid reaction prior to the formation of an imine or enamine. The enhanced reactivity of amines compared to oxyanions (relative second-order rate constants for a tertiary amine, secondary amine, primary amine, and oxyanion of pK_a = 11 are 915:264:100:1 for catalysis of oxaloacetate keto–enol interconversion, compared to 8.1:3.1:2.3:1 for proton abstraction from nitroethane) and the observation of a nonlinear dependence of rate on amine concentration suggests that amine-catalyzed keto–enol interconversion takes place via a carbinolamine intermediate rather than via the well-established simple proton-abstraction mechanism that occurs when the base catalyst is an oxyanion. This is the first example of primary and secondary amine catalyzed labilization of a keto α-hydrogen via a carbinolamine, a more rapid process than the well-known amine-catalyzed labilization of a keto α-hydrogen via imine formation.

We have previously shown that the enolization of oxaloacetic acid does not take place by the well-established base-catalyzed mechanism of eq 1 when the base employed is a tertiary amine.[1]

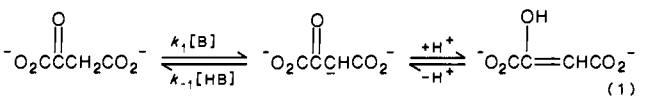

(1)

The observations leading to this conclusion were the following: (1) the second-order rate constant for catalysis by a tertiary amine is as much as 2200 times greater than that for catalysis by an oxyanion of the same pK_a, a rate acceleration too great to be attributed to the enhanced ability of tertiary amines in removing a proton from carbon[2] and (2) enolization exhibits a nonlinear dependence of rate on amine concentration at low concentrations of tertiary amine. To account for these observations we proposed that oxaloacetic acid and tertiary amine react to form a carbinolamine intermediate which yields an enol on reaction with additional amine (eq 2).

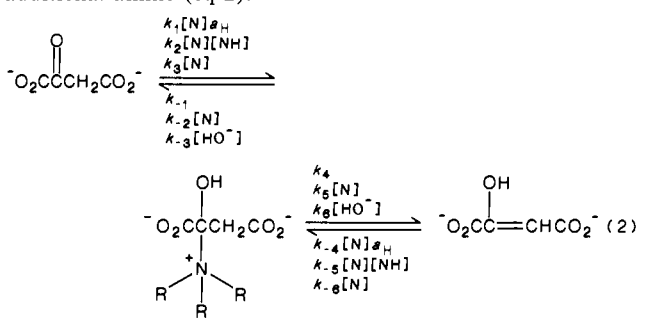

(2)

The present paper describes our investigation of the kinetic behavior of primary and secondary amines with oxaloacetic acid. Although it is well-known that primary and secondary amines react with ketones to form imines and enamines, respectively,[3] and that primary and secondary amines catalyze imine–enamine tautomerism,[4] it has never been determined whether or not such amines are also capable of catalyzing keto–enol tautomerism. We have examined the reaction of oxaloacetic acid with six primary and six secondary amines and have found that the amines initially catalyze keto–enol interconversion in a mechanism similar to that proposed for tertiary amines, then subsequently form an imine or enamine.

Experimental Section

Materials. Oxaloacetic acid (Aldrich) was recrystallized twice from a 50/50 mixture of acetone and benzene. Anal. Calcd for $C_4H_4O_5$: C, 36.38; H, 3.05. Found: C, 36.19; H, 3.09. The amines employed were of the best available commercial grade and were used without further purification. All solids were dried in a vacuum desiccator over P_2O_5.

Buffer Solutions. The amine–amine hydrochloride buffer solutions were prepared just prior to use by the addition of standardized 1.0 M

(1) Bruice, P. Y. *J. Am. Chem. Soc.* **1983**, *105*, 4982.
(2) Bruice, P. Y. *J. Am. Chem. Soc.* **1984**, *106*, 5959.

(3) (a) Hill, R. L.; Crowell, T. I. *J. Am. Chem. Soc.* **1956**, *78*, 2284; 6425. (b) Santerre, G. M.; Hansrote, C. J., Jr.; Crowell, T. I. *J. Am. Chem. Soc.* **1958**, *80*, 1254. (c) McLeod, R. K.; Crowell, T. I. *J. Org. Chem.* **1961**, *26*, 1084. (d) Cordes, E. H.; Jencks, W. P. *J. Am. Chem. Soc.* **1962**, *84*, 832. (e) Layer, R. W. *Chem. Rev.* **1963**, *63*, 489. (f) Crowell, T. I.; Bell, C. E., Jr.; O'Brien, D. H. *J. Am. Chem. Soc.* **1964**, *86*, 4973. (g) Martin, R. B. *J. Phys. Chem.* **1964**, *68*, 1369. (h) Jencks, W. P. *Progress in Physical Organic Chemistry*; Cohen, S. G., Streitweiser, A., Jr., Taft, R. W., Eds.; Interscience: New York, 1964; Vol. 2, p 63. (i) Sollenberger (Bruice), P. Y.; Martin, R. B. *The Chemistry of the Amino Group*; Patai, S., Ed.; Interscience: New York, 1968; p 349.

(4) (a) Bender, M. L.; Williams, A. *J. Am. Chem. Soc.* **1966**, *88*, 2502. (b) Hine, J.; Menon, B. C.; Jensen, H. J.; Mulders, J. *J. Am. Chem. Soc.* **1966**, *88*, 3367. (c) Hine, J.; Cholod, M. S.; King, R. A. *J. Am. Chem. Soc.* **1974**, *96*, 835. (d) Rose, I. R.; O'Connell, E. L. *J. Biol. Chem.* **1969**, *244*, 126.

0002-7863/89/1511-0962$01.50/0

KOH or 1.0 M HCl to the amine hydrochloride or free amine. All buffer solutions were maintained at μ = 0.5 (KCl) and contained 1×10^{-4} M EDTA. The reaction of oxaloacetic acid with each amine was investigated at from 4 to 10 different pH values; all pH values were within ±1 of the ammonium ion pK_a, allowing the amine to act as its own buffer. A minimum of five serially diluted buffer solutions were employed at each pH. The pHs of the serially diluted solutions agreed within 0.02 pH unit. The pK_as of the amines employed were determined by half-neutralization at 30 °C and μ = 0.5. Readings of pH were determined on a Radiometer Type 26 pH meter.

Kinetic Measurements. All kinetic determinations were carried out in doubly glass-distilled water containing 10^{-4} M EDTA to sequester any extraneous metal ions, with μ = 0.5 (KCl). Occasional kinetic determinations were carried out in the absence of EDTA to confirm that EDTA had no effect on any of the rate processes observed. All rate constants were determined at 30.0 ± 0.2 °C.

Reactions were carried out under the pseudo-first-order conditions of $[\text{buffer}]_T \gg [\text{oxaloacetic acid}]$; after mixing of the solution, the final concentration of oxaloacetic acid in the kinetic solution was 6.0×10^{-5} M. All spectrophotometers were thermostated. Reaction rates were determined by monitoring the change in absorbance at 270 nm except in the case of the slowest of the reactions observed with oxaloacetic acid and primary or secondary amines, in which case the absorbance change was monitored at 255 nm. Rate constants for enolization and for imine formation were determined with a Durrum-110 stopped-flow spectrophotometer interfaced to a North-Star microcomputer; rate constants for imine decarboxylation were determined with a Perkin-Elmer Lambda 3 spectrophotometer. Reactions were carried out by mixing amine buffer with oxaloacetic acid equilibrated at either pH 12.3 or pH 2.2; thus when the oxaloacetic acid was mixed with buffer, the reactions occurring after either a rapid decrease or a rapid increase in pH could be monitored. Most of the experiments were carried out with oxaloacetic acid initially equilibrated at pH 12.3; results obtained by employing the acid equilibrated at pH 2.2 were less satisfactory because of complications due to keto–hydrate interconversion. To minimize pH changes upon mixing in the stopped-flow experiments, uneven (1:5) mixing cylinders were used with oxaloacetic acid in the smaller cylinder and amine buffer in the larger. The relative volumes of the mixing cylinders and the dead time of the spectrophotometer were checked by mixing 0.1 M $Fe(NO_3)_3$ in 0.1 N H_2SO_4 (large cylinder) and 0.05 M KSCN (small cylinder) solutions; the dead time was found to be less than 4 ms.

Calculation of the rate constants was done with (1) the stopped-flow spectrophotometer interfaced to a North-Star microcomputer for data digitation and storage employing an On-Line Systems 3820 stopped-flow program and (2) manual digitation of rate traces using a Hewlett-Packard 9820A computer/9864A digitizer. All observed rate constants are the mean of at least three determinations. Calculation of least-squares slopes and intercepts and generation of the theoretical pH–rate profiles were done with the HP 9820A computer.

Results

Ketones in aqueous solution exist in equilibrium with their hydrate and enol forms. The equilibrium distribution of ketone, hydrate, and enol in aqueous solutions of oxaloacetic acid at various values of pH has been reported previously.[5] The percentage of

$$\text{hydrate} \underset{}{\overset{-H_2O}{\rightleftharpoons}} \text{ketone} \rightleftharpoons \text{enol} \underset{+H^+}{\overset{-H^+}{\rightleftharpoons}} \text{enolate} \qquad (3)$$

hydrate in the equilibrium mixture decreases with increasing pH from a value of 95% at pH 0 to 6% at pH 6 and remains unchanged from pH 6 to pH 13. A plot of the equilibrium absorbance at 270 nm of an aqueous solution of oxaloacetate as a function of pH results in a pK_a of 13.04 for the enol tautomer.[1] Only the enol tautomer and the enolate anion absorb light at this wavelength; the keto tautomer and the hydrate evidence no significant absorbance.

The rates of reaction of primary and secondary amines with oxaloacetic acid were determined by mixing amine buffer with oxaloacetic acid that was equilibrated at pH 12.3 and following the change in absorbance at 270 nm. Upon mixing, the pH of the solution immediately changes to that of the amine buffer (pH 6–11). Since the percentage of hydrate remains constant from pH 6 to pH 12.3, no complication is introduced into the kinetics from perturbation of the keto–hydrate equilibrium. In Figure 1

(5) (a) Table I in ref 1. (b) Kokesch, F. C. *J. Org. Chem.* **1976**, *41*, 3593. (c) Emly, M.; Leussing, D. L. *J. Am. Chem. Soc.* **1981**, *103*, 628.

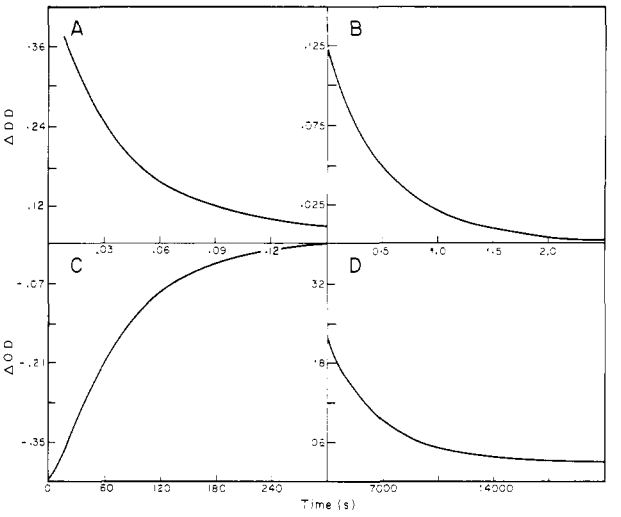

Figure 1. (A–C) Absorbance changes for the three rate processes observed under stopped-flow conditions when oxaloacetic acid equilibrated at pH 12.3 is mixed with a 5-fold excess of 0.06 M ethanolamine buffer at pH 10.33: (A) data were collected during the first 0.15 s after mixing; (B) the solutions were mixed and allowed to equilibrate for 0.15 s, and data were collected during the subsequent 2.5 s; (C) the solutions were mixed and allowed to equilibrate for 7 s and data were collected during the next 300 s. The lines were computer generated through the experimental data points and give rise to rate constants of 25.7, 1.83, and 1.45 $\times 10^{-2}$ s^{-1}, respectively; (D) the absorbance change associated with the fourth rate process obtained for the reaction of oxaloacetic acid with 0.06 M ethanolamine buffer at pH 10.33 ($k_{obsd} = 1.55 \times 10^{-4}$ s^{-1}).

are shown the four rate processes evidenced when oxaloacetic acid is mixed with ethanolamine buffer at pH 10.33. Figure 1A–C shows the three successive rate processes observed with a stopped-flow spectrophotometer: Figure 1A shows data collected during the first 0.15 s after mixing, Figure 1B shows data collected during the subsequent 2.5 s, and in Figure 1C are data obtained between 7 and 300 s after mixing. In Figue 1D is shown the absorbance change associated with a much slower reaction that is observed when the reaction is monitored on a Perkin-Elmer recording spectrophotometer.

The first of the four rate processes (Figure 1A) is associated with a significant decrease in absorbance, about 3 times greater than that for the second rate process. The reaction is observed only when oxaloacetic acid equilibrated at pH 12.3 is mixed with buffered amine to give a solution of pH equal to that of the buffered amine solution (hereafter referred to as a pH-decrease experiment); it is not observed when oxaloacetic acid equilibrated at pH 2.2 is mixed with buffered amine to give a solution of pH equal to that of the buffered amine solution (hereafter referred to as a pH-increase experiment). Plots of k_{obsd} vs $[N]_T$ for the first rate process (Figure 2) show a first-order dependence of rate on amine concentration. When the slopes of such plots are divided by the fraction of the amine buffer present as ammonium ion, $a_H/(K_a + a_H)$, constant second-order catalytic rate constants are obtained, suggesting that the reaction is subject to general acid catalysis. The observed rate constants can, therefore, be expressed as in eq 4, where k_{ly} is the rate of the lyate species catalyzed

$$k_{obsd} = k_{ly} + k_{ga}\,[a_H/(K_a + a_H)][N]_T \qquad (4)$$

reaction, K_a is the acid-dissociation constant of the buffer, a_H is the hydrogen ion activity determined at the glass electrode, $[N]_T$ is the total concentration of amine, i.e., [NH] + [N], and k_{ga} is the second-order rate constant for general-acid catalysis. Values of k_{ga} are given in Table I. This initial reaction is observed only when oxaloacetic acid reacts with primary or secondary amines of $pK_a > 9.5$; it occurs too rapidly to be observed with less basic amines (i.e., more acidic ammonium ions). The logs of the k_{ga} values of eq 4 are plotted vs the pK_a of the amine in the inset to Figure 3. These plots result in Brønsted α values of −0.63 for the reaction of oxaloacetic acid with primary amines and −0.65 for the reaction with secondary amines.

Table I. Second-Order Rate Constants (M^{-1} s^{-1}) for the Reaction of Primary and Secondary Amines with Oxaloacetic Acid

amines	pK_a	k_{ga}	k_{ga}'	k_{gb}'	k_{ga}''	k_{gb}''	k_{ga}'''
primary							
ethylamine	10.74	1160		89.0		9.33×10^{-1}	2.49×10^{-3}
methylamine	10.67	1490		128	7.59×10^{-1}	1.21	5.52×10^{-3}
ethanolamine	9.57	6750		27.5	1.35×10^{-1}	3.48×10^{-1}	9.58×10^{-3}
arginine	9.05			16.1	1.60×10^{-1}		1.12×10^{-2}
tris	8.11			3.56			
glycine ethyl ester	7.39			1.80			2.28×10^{-2}
secondary							
piperidine	11.23	1700		413			7.95×10^{-5}
dimethylamine	10.88	2510		538			2.59×10^{-4}
2-(methylamino)ethanol	9.89	12300		177			
ethyl *N*-piperazinecarboxylate	8.46			52.6			7.85×10^{-4}
1-piperazinecarboxaldehyde	8.05			33.8			1.10×10^{-3}
piperazine	5.82		8.8[a]	9.57			6.85×10^{-3}[a]

[a] The reported value is one-half of the observed value due to the presence of two acidic groups.

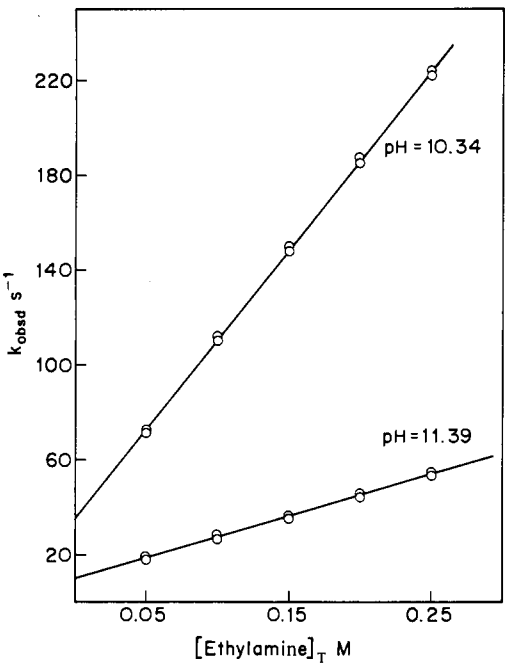

Figure 2. Plots of the observed first-order rate constants for the first of four successive rate processes observed for the reaction of oxaloacetic acid with ethylamine vs the total concentration of ethylamine at two hydrogen ion concentrations.

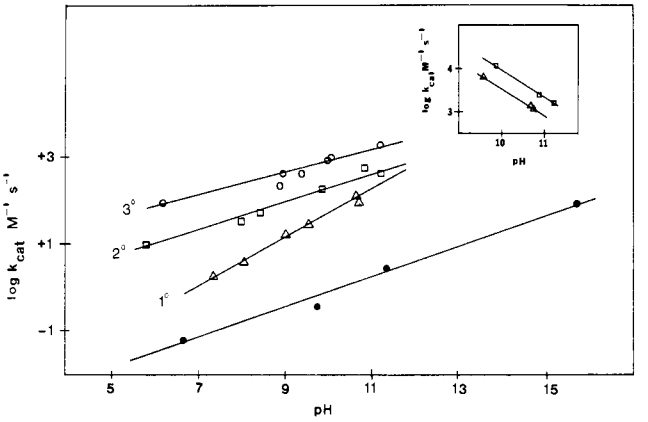

Figure 3. Brønsted plots obtained for keto–enol interconversion of oxaloacetic acid catalyzed by tertiary amines (○), secondary amines (□), primary amines (△), and oxyanions (●); β = 0.24, 0.33, 0.54, and 0.32, respectively. Inset: Brønsted plots for the initial rapid general-acid-catalyzed reaction obtained with secondary amines (□) and primary amines (△); α = −0.65 and −0.63, respectively.

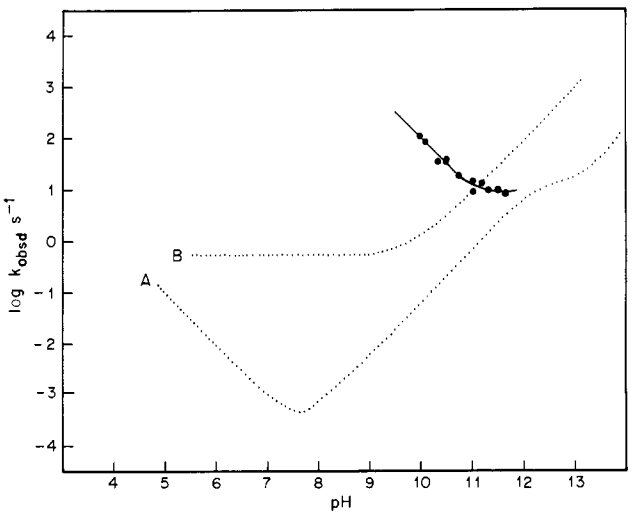

Figure 4. Dotted lines give the pH–rate profiles for: (A) keto–enol interconversion of oxaloacetic acid in the presence of lyate species; (B) keto–hydrate interconversion of oxaloacetic acid in the presence of lyate species. The solid circles are intercepts of buffer-dilution plots obtained for the first rate process evidenced in the reaction of oxaloacetic acid with primary and secondary amines.

Three pH–rate profiles are shown in Figure 4. One (line A) is the pH–rate profile for keto–enol interconversion of oxaloacetic acid via the mechanism of eq 1; rate constants for the establishment of this pH–rate profile were obtained from rates determined in the presence of lyate species and from intercepts of buffer-dilution plots extrapolated to zero buffer concentration by employing oxyanion buffers.[1] The second pH–rate profile (line B) is that for keto–hydrate interconversion of oxaloacetic acid. Rate constants for keto–hydrate interconversion could not be obtained with lyate species or oxyanion buffers since under such conditions keto–hydrate interconversion is faster than keto–enol interconversion and neither the ketone nor the hydrate evidence any significant spectral absorbance. Rate constants for the dehydration pH–rate profile were obtained from the intercepts of buffer-dilution plots obtained for the reaction of oxaloacetic acid with tertiary amines.[1] In the presence of tertiary amine catalysts, keto–enol interconversion is faster than keto–hydrate interconversion. Thus the rate of keto–hydrate interconversion could be monitored by the change in enol absorbance that occurs as the keto–enol equilibrium shifts to accommodate the slower, and consequently rate-limiting, change in the keto–hydrate equilibrium.[1] To measure the rate of keto–hydrate interconversion, oxaloacetic acid equilibrated at pH 2.2 was added to the buffered tertiary amine; keto–hydrate interconversion was not detected in identical experiments employing oxaloacetic acid equilibrated at pH 12.3 since there is no change in the percentage of hydrate from pH 6 to pH 13.

Also in Figure 4 are plotted the logs of the intercept values (solid circles) obtained in this study by extrapolating the buffer dilution plots for the first rate process evidenced in the reaction of primary and secondary amines with oxaloacetic acid to zero buffer con-

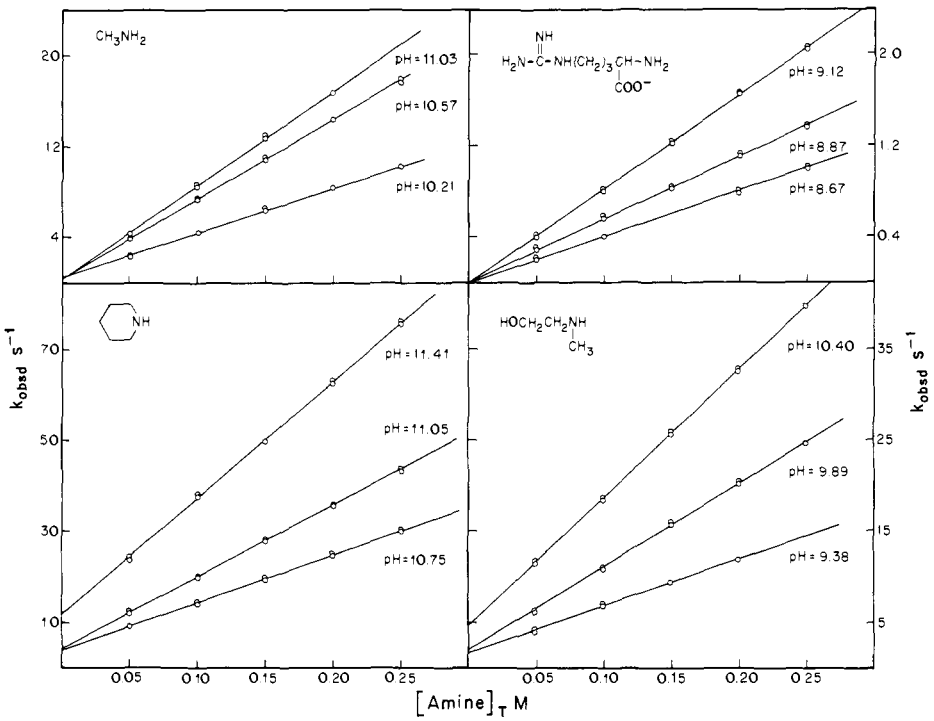

Figure 5. Plots of the observed first-order rate constants for the second rate process evidenced in the reaction of oxaloacetic acid with primary and secondary amines vs the total concentration of amine. Data are shown for two primary amines (methylamine and arginine) and two secondary amines (piperidine and 2-(methylamino)ethanol).

centration (i.e. buffer dilution plots such as those shown in Figure 2). The solid line drawn through these intercept values is defined by eq 5, where k_{obsd} is the value of the intercept at zero amine

$$k_{obsd} = k_H a_H + k_0 \quad (5)$$

concentration and a_H is the hydrogen ion activity determined at the glass electrode: $k_H = 1.10 \times 10^{12}$ M^{-1} s^{-1} and $k_0 = 9.10$ s^{-1}. The k_{obsd} term of eq 5 is equivalent to the k_{ly} term of eq 4.

The second rate process (Figure 1B) observed in the reaction of oxaloacetic acid with primary and secondary amines gives rise to buffer-dilution plots such as those shown in Figure 5. All the amines, except piperazine, evidence only general-base catalysis; piperazine exhibits both general-base and general-acid catalysis. The observed rate constants can, therefore, be expressed as in eq 6 and 7. Plots of k_{obsd} vs $[B]_T$ (such as those in Figure 5) give

$$k_{obsd} = k_{ly}' + k_{gb}' [K_a/(K_a + a_H)][B]_T \quad (6)$$

$$k_{obsd} = k_{ly}' + k_{gb}' [(K_a/K_a + a_H)][B]_T + k_{ga}' [a_H/(K_a + a_H)][B]_T \quad (7)$$

slopes that, when divided by the mole fraction of buffer present in the basic form, $K_a/(K_a + a_H)$, give values of k_{gb}' if only general-base catalysis is operative and values of $k_{gb}' + k_{ga}' a_H/K_a$ if both general-base and general-acid catalysis occur. In the latter case, values of k_{gb}' and k_{ga}' can be obtained from the intercepts and slopes, respectively, of secondary plots of slope/$[K_a/(K_a + a_H)]$ vs a_H/K_a. Values of k_{gb}' thus obtained for the reaction of oxaloacetic acid with primary and secondary amines are plotted in Figure 3 together with the general base catalytic constants obtained previously for the reaction of oxaloacetic acid with tertiary amines and oxyanions.

Although most of the data for the second rate process was obtained by mixing oxaloacetic acid equilibrated at pH 12.3 with the buffered amine solution, rate constants for the second rate process were also obtained by mixing oxaloacetic acid equilibrated at pH 2.2 with buffered amine. Observed first-order rate constants obtained under both pH-decrease and pH-increase conditions are plotted in Figure 6 for the second rate process evidenced in the reaction of oxaloacetic acid with ethanolamine at pH 9.57. The pH-decrease and pH-increase experiments are both characterized by decreasing absorbance; rate constants were more difficult to

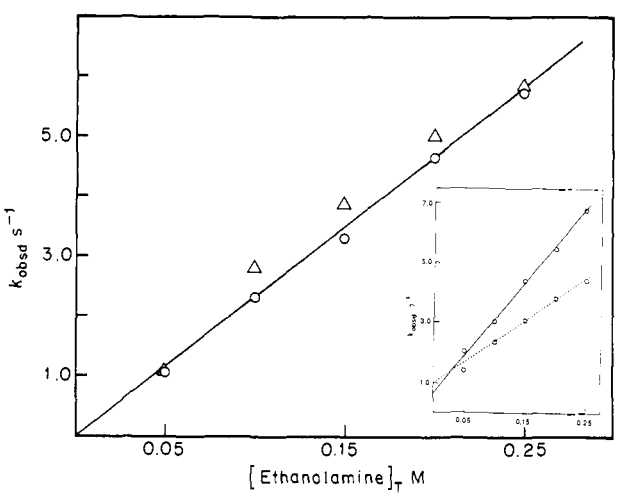

Figure 6. Observed first-order rate constants for the ethanolamine-catalyzed enolization of oxaloacetic acid (second rate process) vs the total concentration of ethanolamine buffer: (△) rate constants obtained upon mixing oxaloacetic acid equilibrated at pH 2.2 with ethanolamine buffer at pH 9.57; (○) rate constants obtained upon mixing oxaloacetic acid equilibrated at pH 12.3 with ethanolamine buffer at pH 9.57. Inset: The solid line represents rate constants obtained for keto–enol interconversion (second rate process) with ethanolamine buffer at pH 10.49. The dashed line represents rate constants obtained for keto–hydrate interconversion with ethanolamine buffer at pH 10.49.

obtain for the pH-increase experiments because of interference from a rate process that is not observed in the pH-decrease experiments; thus most of the experiments carried out in this study were done under pH-decrease conditions. In the reaction of oxaloacetic acid with ethanolamine under pH-decrease conditions the second rate process with a k_{gb} of 27.5 M^{-1} s^{-1} (Figure 6) is followed by a slower reaction with a k_{gb} of 3.48×10^{-1} M^{-1} s^{-1} that is characterized by increasing absorbance (the third rate process); under pH-increase conditions the second rate process with a k_{gb} of 27.5 M^{-1} s^{-1} (Figure 6 and the solid line in the inset to Figure 6) is followed by two reactions both evidencing increasing absorbance with time. The first of these, with a k_{gb} of 15 M^{-1} s^{-1} (dashed line in the inset to Figure 6), is not observed in the

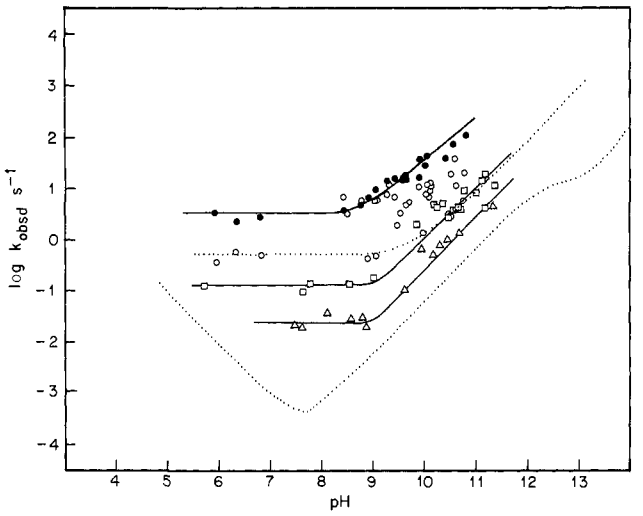

Figure 7. Dotted lines correspond to the two pH–rate profiles of Figure 4. Intercepts of amine buffer dilution plots at zero amine concentration obtained for the second rate process observed upon mixing oxaloacetic acid equilibrated at pH 12.3 with primary amines (△), secondary amines (□), tertiary amines (○), and upon mixing oxaloacetic acid equilibrated at pH 2.2 with tertiary amines (●).

pH-decrease experiments; the second (k_{gb} = 3.48 × 10^{-1} M^{-1} s^{-1}) is identical with the third rate process observed in the pH-decrease experiments. Similarly, in the reaction of oxaloacetic acid with the secondary amine dimethylamine under pH-increase conditions, the second rate process (k_{gb} = 538 M^{-1} s^{-1}) is followed by a reaction (k_{gb} = 58 M^{-1} s^{-1}) evidencing increasing absorbance which is not observed under pH-decrease conditions and which is followed by the third rate process.

The logs of the intercepts of the buffer-dilution plots at zero amine concentration for the second rate process evidenced in the reaction of oxaloacetic acid with primary and secondary amines (plots such as those shown in Figure 5) are plotted in Figure 7 together with the intercepts obtained from similar experiments for the reaction of oxaloacetic acid with tertiary amines. Also in Figure 7 are shown intercept values obtained for the reaction of oxaloacetic acid with tertiary amines in experiments in which oxaloacetic acid was equilibrated at pH 2.2 rather than an pH 12.3. The solid lines of Figure 7 were generated from eq 8, where

$$k_{obsd} = k_0 + k_{HO}K_w/a_H \quad (8)$$

pK_w = 13.83, and k_0 = 2.29 × 10^{-2} s^{-1} and k_{HO} = 1.65 × 10^3 M^{-1} s^{-1} for primary amines and k_0 = 1.26 × 10^{-1} s^{-1} and k_{HO} = 6.46 × 10^3 M^{-1} s^{-1} for secondary amines.

Although the amine buffer-dilution plots for the second rate process (Figure 5) are linear, indicating a first-order dependence of rate on amine concentration, that linearity is not maintained if the plots are extended to very low amine concentrations with 0.2 M carbonate buffer to maintain constant pH. In Figure 8 is shown a plot of the observed first-order rate constants for the reaction (second rate process) of oxaloacetic acid with dimethylamine, determined over a concentration range of 0.001–0.25 M $[N]_T$. All the amines listed in Table I exhibit similar behavior. The apparent first-order dependence of rate on amine concentration exhibited in Figure 5, which gives rise to intercept values at zero amine concentration that are very much larger than would be expected for the lyate species catalyzed reaction at the given pH, does not hold up when the buffer-dilution plots are extended to include rate constants obtained at low concentrations of amine. There is a significant negative deviation from the line established for the first-order amine dependence with the rate constants approaching the value for carbonate-catalyzed enolization via the mechanism of eq 1 at zero amine concentration.

The third rate process evidenced in the reaction of oxaloacetic acid with primary and secondary amines, unlike the first two rate processes, is characterized by increasing absorbance (Figure 1C). Whether oxaloacetic acid is initially equilibrated at pH 2.2 or at

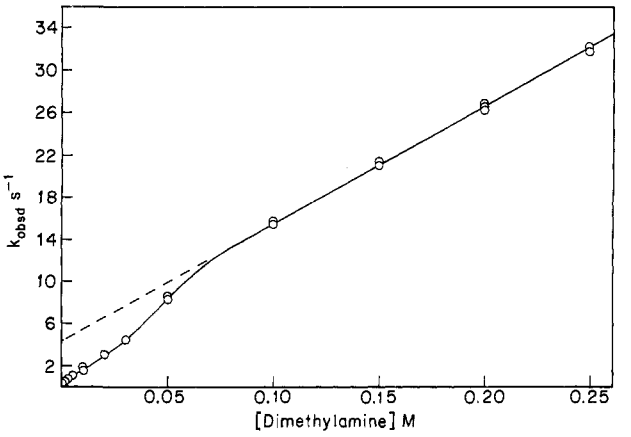

Figure 8. Observed first-order rate constants for the reaction of oxaloacetic acid (second rate process) with dimethylamine vs the total concentration of dimethylamine at pH 10.28; amine solutions <0.1 M contain 0.2 M carbonate at pH 10.28.

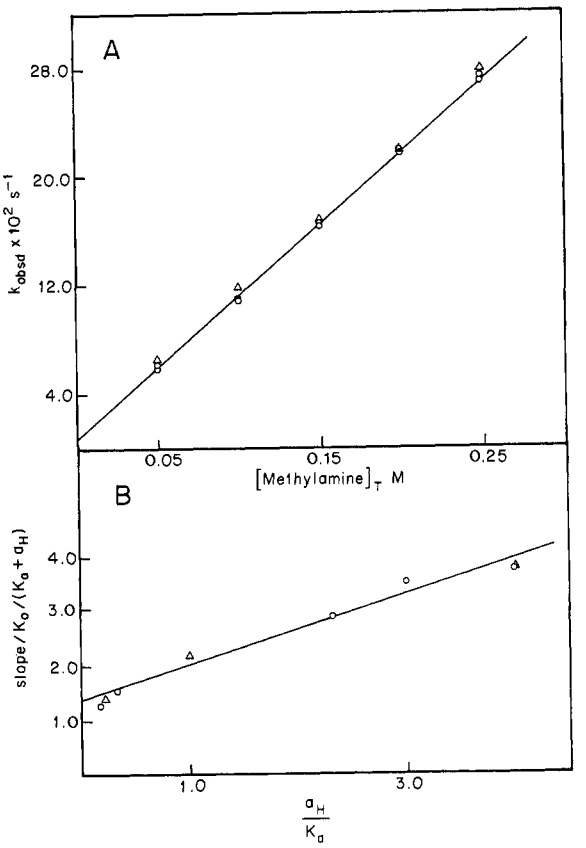

Figure 9. (A) Observed first-order rate constants for the reaction of oxaloacetic acid (third rate process) with methylamine vs the total concentration of methylamine at pH 11.43: (△) rate constants obtained upon mixing oxaloacetic acid equilibrated at pH 2.2 with methylamine buffer at pH 11.43; (○) rate constants obtained upon mixing oxaloacetic acid equilibrated at pH 12.3 with methylamine buffer at pH 11.43. (B) Plot of the slopes of buffer-dilution plots for the reaction of oxaloacetic acid with methylamine (third rate process) divided by the mole fraction of the buffer present in the basic form vs the mole fraction of buffer present in the acidic form divided by the mole fraction of buffer present in the basic form: (△) data obtained from pH-increase experiments; (○) data obtained from pH-decrease experiments.

pH 12.3 before it is added to the buffered amine solution has no effect on the observed rate constant for this third rate process; rate constants under both conditions are equally easy to obtain and give rise to identical values. In Figure 9A are plotted the rate constants for the third rate process evidenced in the reaction of oxaloacetic acid with methylamine under both pH-increase and pH-decrease conditions.

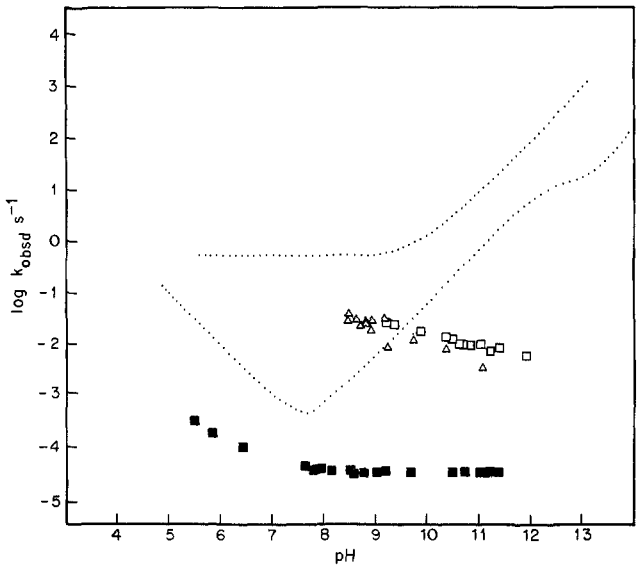

Figure 10. Dotted lines correspond to the two pH–rate profiles of Figure 4. Intercepts of the amine buffer dilution plots at zero amine concentration for the third rate process evidenced in the reaction of oxaloacetic acid with primary amines (△), observed first-order rate constants for the third rate process evidenced in the reaction of oxaloacetic acid with secondary amines (□), and intercepts of the amine buffer dilution plots at zero amine concentration for the fourth rate process observed in the reaction of oxaloacetic acid with secondary amines (■).

For the reaction of oxaloacetic acid with primary amines, the nature of the catalysis observed for the third rate process depends on the pK_a of the amine. Ethylamine, the most basic of the primary amines investigated (pK_a = 10.74), evidences only general-base catalysis; thus the observed rate constants can be expressed by eq 6. Methylamine and ethanolamine (pK_a = 10.67 and 9.57, respectively) evidence both general-base and general-acid catalysis (as described by eq 7); the catalytic constants must be obtained from secondary plots of slope/$[K_a/(K_a + a_H)]$ vs a_H/K_a. The secondary plot from which the general base and general acid catalytic constants for methylamine were obtained is shown in Figure 9B. It should be noted that some of the points on the secondary plot were obtained from pH-increase experiments while others were obtained from pH-decrease experiments. Arginine (pK_a = 9.05) exhibits only general-acid catalysis (as described by eq 4). This third rate process is not observed at all with more weakly basic primary amines. The general acid and general base catalytic rate constants (k_{ga}'' and k_{gb}'') obtained for this third rate process are given in Table I. The logs of the intercept values of the buffer-dilution plots extrapolated to zero buffer concentration for the third rate process observed in the reaction of oxaloacetic acid with primary amines are plotted in Figure 10.

In the case of secondary amines, the third rate process is not subject to general acid–base catalysis; the observed rate constants are independent of amine concentration. Similar to what was observed with primary amines, the third rate process is not observed at all with the least basic secondary amines, piperazine (pK_a = 5.82) and 1-piperazinecarboxaldehyde (pK_a = 8.05). With ethyl *N*-piperazinecarboxylate (pK_a = 8.46), the third rate process is observed only if the pH of the buffer system is >9.2. The absorbance change for the third rate process with secondary amines is very much smaller than that for the third rate process with primary amines, making it difficult to obtain accurate values for the observed rate constants. Those observed rate constants that were obtained for the third rate process evidenced in the reaction of oxaloacetic acid with secondary amines are plotted in Figure 10.

The fourth rate process is characterized by decreasing absorbance (Figure 1D); this slow reaction of oxaloacetic acid is observed with both primary and secondary amines and is associated with only general-acid catalysis. Values of k_{ga}''' for this reaction are given in Table I. The logs of the intercept values of the buffer-dilution plots for the fourth rate process observed in the reaction of oxaloacetic acid with secondary amines are plotted in Figure 10. The slopes of the buffer-dilution plots for the fourth rate process evidenced in the reaction of oxaloacetic acid with primary amines are too steep to allow accurate intercept values to be obtained; they are the same order of magnitude as those obtained with secondary amines.

Scheme I

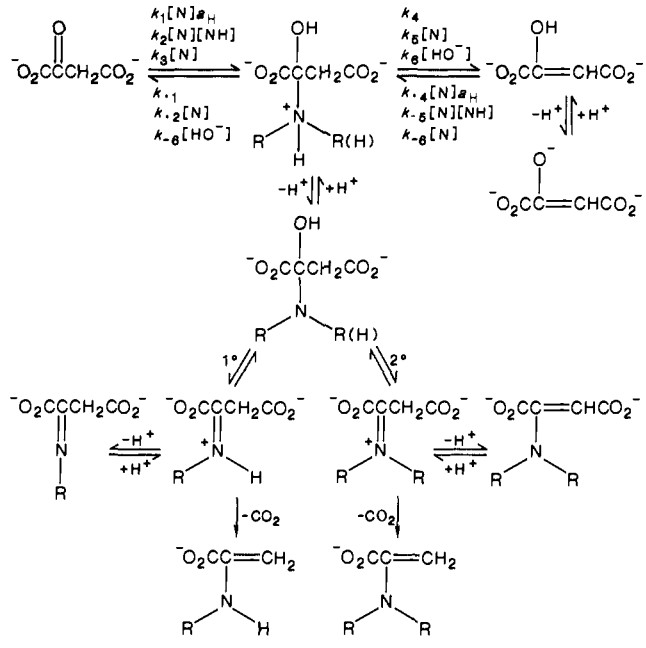

Discussion

The results obtained in this study of the reaction of oxaloacetic acid with primary and secondary amines can be best explained by the sequence of reactions shown in Scheme I. Primary and secondary amines catalyze keto–enol interconversion via the nucleophilic addition–elimination mechanism that we proposed previously for tertiary amine catalyzed enolization.[1] The nucleophilic addition–elimination mechanism involves attack of amine on the ketone carbonyl group to form a carbinolamine intermediate. A second molecule of amine reacts with the carbinolamine via an E2 type mechanism to give enol by elimination of a proton and neutral amine. Loss of water from the carbinolamine results in the formation of an imine in the case of primary amines and formation of an enamine in the case of secondary amines. Both the imine and enamine subsequently lose CO_2 to give an α,β-unsaturated secondary amine and an α,β-unsaturated tertiary amine, respectively. The sequence of reactions observed in Scheme I result in the observation of four rate processes for the reaction of oxaloacetic acid with primary amines and secondary amines.

The first rate process (Figure 1A) evidenced in the reaction of oxaloacetic acid with both primary and secondary amines is characterized by a significant decrease in absorbance and is subject to catalysis by general acids (Figure 2). The reaction is very fast (k_{ga} of Table I) and can be observed only when the pK_a of the ammonium ion is >9.5; in the case of more strongly acidic ammonium ions the reaction occurs too rapidly to be detected on the stopped-flow time scale. This reaction can be attributed to protonation of the enolate anion by ammonium ion. To initiate the reaction, oxaloacetic acid equilibrated at pH 12.3 is added to the buffered amine solution. At pH 12.3 about 20% of the equilibrium mixture of keto, hydrate, and enol is comprised of enol and enolate; since the pK_a of the enol is 13.04,[1] 15% of enol + enolate exists as enolate. The enolate anion absorbs very strongly at 270 nm; thus, protonation of this species would be in agreement with the significant decrease in absorbance that is observed. Attributing this first rate process to enolate protonation explains why the reaction is observed when a solution of oxaloacetic acid equilibrated at pH 12.3 is mixed with a buffered amine solution, resulting in a sudden decrease in pH to that of the buffered amine solution

(a pH-decrease experiment), and is not observed when a solution of oxaloacetic acid equilibrated at pH 2.2 is mixed with a buffered amine solution, resulting in a sudden increase in pH to that of the buffered amine solution (a pH-increase experiment). The reaction is associated with a hydrogen ion catalyzed term, $k_H = 1.10 \times 10^{12}$ M^{-1} s^{-1}, and a noncatalyzed term, $k_0 = 9.10$ s^{-1} (eq 5).

The hydrogen ion catalyzed term is clearly too large to be attributed to hydronium ion protonation of enolate but may be attributed to intramolecular protonation of the enolate anion by a carboxyl group of oxaloacetic acid (I). The pK_as of the carboxyl

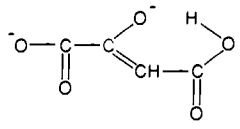

I

groups of the enol tautomer of oxaloacetic acid have been reported to be 1.89 and 3.72.[6] The kinetic expression for protonation of the enolate anion may be described by the rate law of eq 9, where

$$k_{obsd} = k_H'[a_H/(K_a' + a_H)] + k_0'[H_2O] + k_{ga}[a_H/(K_a + a_H)][N]_T \quad (9)$$

k_H' is the rate of intramolecular protonation by the carboxyl group, k_0' and k_{ga} are the rates of protonation by water and ammonium ion, respectively, and K_a' and K_a are the acid-dissociation constants for the carboxyl group and the ammonium ion, respectively. In the investigated pH range, $K_a' \gg a_H$, therefore eq 9 can be simplified to give eq 10. The k_H'/K_a' and $k_0'[H_2O]$ terms of eq 10

$$k_{obsd} = k_H'a_H/K_a' + k_0'[H_2O] + k_{ga}[a_H/(K_a + a_H)][N]_T \quad (10)$$

correspond to the k_H and k_0 terms of eq 5. With pK_a = 3.72, k_H' is equal to 2.10×10^8 M^{-1} s^{-1}, a reasonable value for intramolecular general acid catalysis. The observed rate constant of 9.10 s^{-1} for water-catalyzed protonation of the enolate anion can be compared to the value of 6.70 s^{-1} obtained for the same reaction in the study of the reaction of oxaloacetic acid with tertiary amines.[1] Rate constants ranging from 1.3 to 8.0 s^{-1} have been reported for water-catalyzed protonation of a series of α-substituted ethyl acetoacetates.[7]

The second rate process (Figure 1B) evidenced in the reaction of primary and secondary amines with oxaloacetic acid is characterized by decreasing absorbance. This second rate process is observed in both pH-decrease experiments and in pH-increase experiments; identical observed rate constants are obtained under both conditions (Figure 6). This reaction can be attributed to keto–enol interconversion. At pH 12.3 the [enol]/[ketone] ratio is ~0.25, and at pH 2.2 the ratio is ~0.30, while at the pH of the buffered amine solutions the ratio is ~0.15; thus decreasing absorbance is observed in both sets of experiments as a result of a shift in the keto–enol equilibrium toward the nonabsorbing keto tautomer.[1]

In the pH-decrease experiments keto–enol interconversion is followed by a slower reaction characterized by increasing absorbance, which we have referred to as the third rate process. In the pH-increase experiments keto–enol interconversion is followed by two rate processes both evidencing an increase in absorbance with time. The second of these two rate processes that follow keto–enol interconversion is identical with the single reaction evidencing increasing absorbance that is observed in the pH-decrease experiments and which we have designated as the third rate process. The first of the two rate processes that follow keto–enol interconversion is attributable to keto–hydrate interconversion. Keto–hydrate interconversion is not observed in the pH-decrease experiments since the percentage of hydrate remains constant from pH 12.3 to pH 6.

At pH 2.2 the [enol]/[ketone] ratio is ~0.30 and the [hydrate]/[ketone] ratio is >1.0.[5] When acidic oxaloacetic acid is mixed with a more basic solution so that the final pH is between 7 and 11, where the [enol]/[ketone] ratio is ~0.15 and the [hydrate]/[ketone] ratio is ~0.08, the rate process(es) observed will depend on the relative rates of keto–enol and keto–hydrate interconversion. If keto–enol interconversion is slower than keto–hydrate interconversion, as is the case in the presence of lyate species or oxyanion bases (Figure 7), keto–hydrate interconversion will be spectrally invisible and the only rate process observed will be a reaction characterized by decreasing absorbance due to the conversion of enol to ketone in order to shift the [enol]/[ketone] ratio from 0.30 to 0.15. On the other hand, if keto–enol interconversion is faster than keto–hydrate interconversion, as we have found to be the case in the presence of primary, secondary, or tertiary amines (inset to Figure 6), two reactions will be observed, the first evidencing decreasing absorbance and the second increasing absorbance with time. The initial loss of absorbance as enol is converted to ketone will be followed by the slower conversion of hydrate to ketone as the [hydrate]/[ketone] ratio decreases from >1.0 to 0.08. This normally spectrally unobservable reaction can be monitored by the rate of increase in absorbance due to the rapid formation of enol, which will follow the rate-limiting conversion of hydrate to ketone. The second-order general base catalyzed rate constants of 58 M^{-1} s^{-1} for dimethylamine and 15 M^{-1} s^{-1} for ethanolamine-catalyzed keto–hydrate interconversion are consistent with rate constants obtained previously for tertiary amine catalyzed keto–hydrate interconversion of oxaloacetic acid.[1] Pogson and Wolfe reported a value of 0.48 s^{-1} for the dehydration of oxaloacetic acid in 0.1 M phosphate at 20 °C;[8] extrapolation of the ethanolamine buffer dilution plots to zero amine concentration results in a pH-independent water-catalyzed rate constant of 0.94 s^{-1} at 30 °C (inset to Figure 6).

Two observations confirm the assignment of the second rate process to keto–enol interconversion: (1) the reaction is characterized by decreasing absorbance in both the pH-increase and pH-decrease experiments, as required by the [keto]/[enol] composition at pH 2.2, at pH 12.3, and at the pH of the amine buffer solutions; (2) in the pH-increase experiments the second rate process is followed by keto–hydrate interconversion which is followed by the third rate process, while in the pH-decrease experiments the second rate process is followed directly by the third rate process. Only under conditions where keto–enol interconversion is faster than keto–hydrate interconversion can the latter be observed; keto–hydrate interconversion is not observed in the pH-decrease experiments, as predicted by the invariant concentration of hydrate in the pH range 6–12.3.

Representative buffer-dilution plots are shown in Figure 5 for the second rate process evidenced in the reaction of oxaloacetic acid with primary and secondary amines. The observed rate constants exhibit an apparent linear dependence on amine concentration; the slopes of the buffer-dilution plots indicate that keto–enol interconversion is subject only to catalysis by amine free base except in the case of piperazine, where both general base and general acid catalysis are apparent. In Figure 3 are plotted the second-order rate constants for primary amine (△) and secondary amine (□) catalyzed enolization together with the second-order rate constants obtained previously for tertiary amine (○) and oxyanion (●) catalyzed enolization. The second-order rate constants define Brønsted β values of 0.54, 0.33, and 0.24 for primary, secondary, and tertiary amines, respectively, while that for oxyanions is 0.32. Secondary amines were chosen that would give minimum steric effects. The relative slopes of the Brønsted plots for primary, secondary, and tertiary amine catalyzed keto–enol interconversion are in accord with the reactivity–selectivity principle, which states that within a series of similar reactions, reactivity and selectivity should exhibit an inverse correlation; substrates showing high reactivity should be characterized by limited selectivity while those exhibiting low reactivity

(6) Tate, S. S.; Grzybowski, A. K.; Datta, S. P. *J. Chem. Soc.* **1964**, 1372.
(7) Brouillard, R.; Dubois, J. E. *J. Org. Chem.* **1974**, *39*, 1137.
(8) Pogson, C. I.; Wolfe, R. G. *Biochem. Biophys. Res. Commun.* **1972**, *46*, 1148.

should be characterized by a higher selectivity.[9]

The second-order general-base rate constants for amine-catalyzed keto–enol interconversion of oxaloacetic acid are much larger than those for oxyanion catalysis of the same reaction (Figure 3). The relative second-order rate constants for a tertiary amine, secondary amine, primary amine, and oxyanion of $pK_a = 11.0$ are 915:264:100:1. The long-accepted base-catalyzed mechanism for keto–enol interconversion involves simple rate-limiting proton abstraction from carbon (eq 1). Although amines are generally found to be more efficient than oxygen bases of the same pK_a in abstracting a proton from carbon, this greater efficiency is not sufficient to account for the observed reactivity differences between amines and oxygen bases in catalysis of oxaloacetic acid keto–enol interconversion. In a study of base-catalyzed nitroethane ionization, a reaction in which the only mechanism possible is rate-limiting removal of a proton from carbon, the relative second-order rate constants for a tertiary amine, secondary amine, primary amine, and oxyanion of $pK_a = 11.0$ were found to be 8.1:3.1:2.3:1.[10] Thus, on the basis of the magnitude of the second-order catalytic rate constants, it is unlikely that amine-catalyzed keto–enol interconversion of oxaloacetic acid and oxyanion-catalyzed keto–enol interconversion of oxaloacetic acid take place by the same mechanism. It would appear that a considerably more facile mechanism than that of eq 1 is available for amine-catalyzed keto–enol interconversion.

The intercepts of the amine buffer dilution plots of Figure 5 also indicate that a mechanism other than the well-known mechanism of eq 1 is followed when the basic catalyst is an amine. Similar to what was found in the study of tertiary amine catalyzed enolization of oxaloacetic acid, the intercepts of the buffer-dilution plots at zero amine concentration for primary and secondary amine catalyzed enolization do not fall on the pH–rate profile established for lyate species catalyzed enolization (Figure 7). The rate of the water-catalyzed reaction that occurs in the presence of primary amines is 288 times greater, and in the case of secondary amines 52 times greater, than can be attributed to water-catalyzed keto–enol interconversion via the mechanism of eq 1; the specific-base-catalyzed rate constant, k_{HO}, defined by the pH–rate profiles of Figure 7, are 88-fold greater for primary amines and 22-fold greater for secondary amines than the specific-base-catalyzed rate constant for proton abstraction from oxaloacetic acid via the mechanism of eq 1. This suggests that, in the presence of amines, lyate species are operating not on ketone or enol but on a more reactive intermediate.

As a result of these large intercept values, the buffer-dilution plots of Figure 5 were extended to very low concentrations of amine. The results obtained with dimethylamine at pH 10.28 are shown in Figure 8; in order to maintain constant pH, amine solutions that were <0.1 M contained carbonate buffer of pH 10.28. The apparent first-order dependence of rate on amine concentration evidenced by the buffer-dilution plots of Figure 5 is not maintained at low amine concentration. Thus amine-catalyzed keto–enol interconversion apparently follows a rate law that is greater than first-order in amine at low concentrations of amine.

The large second-order rate constants for primary and secondary amine catalyzed keto–enol interconversion of oxaloacetic acid compared to the second-order rate constants for oxygen base catalyzed keto–enol interconversion, the intercepts of the buffer dilution plots that do not fall on the line for lyate species catalyzed enolization, and the non-first-order dependence of rate on amine concentration are similar to what was observed in our earlier study of tertiary amine catalyzed keto–enol interconversion of oxaloacetic acid. These observations led us to propose that in the presence of tertiary amine catalysts enolization of oxaloacetic acid does not take place via the mechanism of eq 1 but instead follows the mechanism of eq 2, which involves the formation of a carbinolamine intermediate. The similar behavior of primary and secondary amines leads to the conclusion that these amines also do not catalyze keto–enol interconversion of oxaloacetic acid via the mechanism of eq 1 but must involve a mechanism similar to that proposed for tertiary amines. This mechanism is shown in Scheme II.

Assumption of steady-state formation of CH^+ results in eq 11, where K_a is the acid-dissociation constant of ammonium ion.

$$k_{obsd} = k_f + k_r = \{(k_2k_5/K_a + k_{-2}k_{-5}/K_a)a_H[N]^3 + (k_2k_4/K_a + k_{-1}k_{-5}/K_a + k_1k_5 + k_{-2}k_{-4})a_H[N]^2 + (k_2k_6K_W/K_a + k_{-3}k_{-5}K_W/K_a + k_3k_5 + k_{-2}k_{-6})[N]^2 + (k_1k_4 + k_{-1}k_{-4})a_H[N] + (k_1k_6K_W + k_{-3}k_{-4}K_W + k_{-1}k_{-6})[N] + (k_3k_6 + k_{-3}k_{-6})K_W[N]/a_H\}/\{(k_{-1} + k_{-2}[N] + k_{-3}K_W/a_H) + (k_4 + k_5[N] + k_6K_W/a_H)\} \quad (11)$$

If one assumes preequilibrium formation of CH^+ in both forward and reverse directions, the mechanism of Scheme II prescribes the rate expression of eq 12, where K_c is the acid-dissociation constant of CH^+.

$$k_{obsd} = k_f + k_r = (k_5K_1a_H[N]^2 + k_4K_1a_H[N] + k_6K_1K_W[N])/(1 + K_1[N](K_c + a_H)) + (k_{-2}a_H[N]^2 + k_{-1}a_H[N] + k_{-3}K_W[N])/(k_4 + [N](K_c + a_H)) \quad (12)$$

The assumption of preequilibrium formation of CH^+ in the forward direction and rate-limiting formation of CH^+ in the reverse direction leads to the rate expression of eq 13, where K_a and K_c are the acid-dissociation constants of ammonium ion and CH^+, respectively.

$$k_{obsd} = k_f + k_r = (k_5K_1a_H[N]^2 + k_4K_1a_H[N] + k_6K_1K_W[N])/(1 + K_1[N](K_c + a_H)) + k_{-5}a_H[N]^2/K_a + k_{-4}a_H[N] + k_{-6}[N] \quad (13)$$

All three assumptions are in agreement with the observation of a non-first-order dependence of rate on amine concentration at low concentrations of amine, a first-order dependence of rate on amine concentration at higher concentrations of amine, and general-base or general-acid and general-base catalysis, depending on amine pK_a. Depending on the magnitude of the individual rate and equilibrium constants, the three rate equations can also account for the pH dependence of the intercepts of the amine buffer dilution plots.

The third rate process (Figure 1C) evidenced in the reaction of oxaloacetic acid with primary and secondary amines was not observed in the study of the reaction of oxaloacetic acid with tertiary amines. This rate process may be attributed to dehydration of the carbinolamine addition compound to give an imine in the case of primary amines and an enamine in the case of secondary amines, reactions that cannot occur if the amine component of the carbinolamine is a tertiary amine. Assignment of the reaction to imine and enamine formation is in agreement with the observation that observed first-order rate constants obtained from pH-decrease experiments are identical with those obtained from pH-increase experiments (Figure 9A) and is also in agreement with the much smaller absorbance change associated with enamine formation compared to imine formation.

In the reaction of oxaloacetic acid with secondary amines, breakdown of the carbinolamine intermediate is not subject to general-acid–base catalysis nor is specific-acid or specific-base catalysis involved. The immonium product that results subsequently loses a proton from the β-carbon in a non-rate-limiting step to give an enamine (eq 14). The observed first-order rate

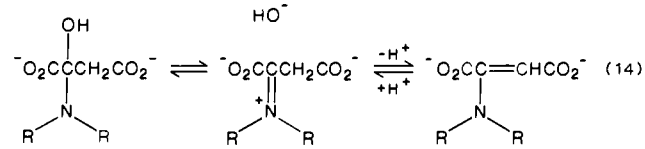

(14)

constants are plotted in Figure 10 (open squares). Since these rate constants refer to collapse of four different carbinolamines, they cannot be compared as a group. They do, however, indicate

(9) (a) Leffler, J. E.; Grunwald, E. *Rates and Equilibria of Organic Reactions*; Wiley: New York, 1963. (b) Giese, B. *Angew. Chem., Int. Ed. Engl.* **1977**, *16*, 125. (c) Pross, A. *Adv. Phys. Org. Chem.* **1977**, *14*, 69. (d) McLennan, D. J. *Tetrahedron* **1978**, *34*, 2331.

(10) Bruice, P. Y., unpublished data.

Scheme II

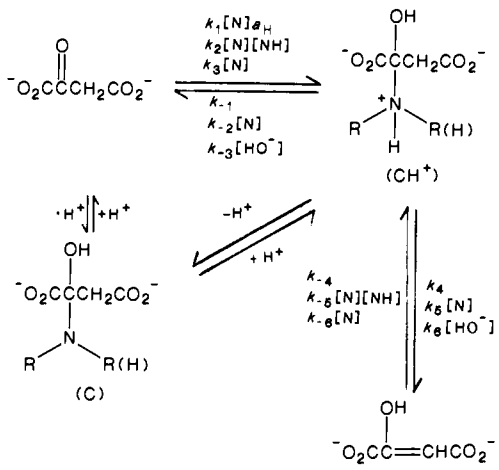

the absence of specific catalysis, and they confirm that the third rate process cannot be attributed to keto–enol interconversion via the mechanism of eq 1 or to keto–hydrate interconversion.

Dehydration of the carbinolamine formed in the reaction of oxaloacetic acid with primary amines is subject to general-acid catalysis and general-base catalysis, depending on the pK_a of the amine. Possible mechanisms for the general catalysis are shown in eq 15, although there are other kinetically equivalent mecha-

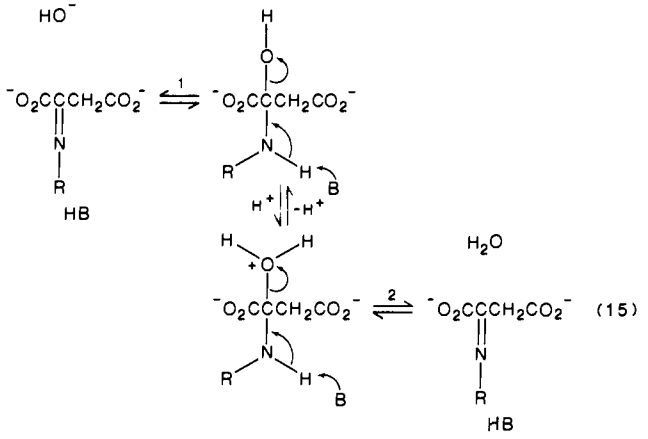

nisms as well. Dehydration of the carbinolamine via mechanism 1 would appear as general-base catalysis, while dehydration via mechanism 2 would appear as general-acid catalysis. In Figure 10 (open triangles) are plotted the intercept values obtained by extrapolation of the buffer-dilution plots for amine-catalyzed imine formation to zero amine concentration; the intercept values pertain to imine formation from four different carbinolamines.

As amine basicity decreases, the rate of the general-base-catalyzed second rate process decreases and the rate of the predominantly acid-catalyzed third rate process increases. Thus the most weakly basic of the primary and secondary amines employed in this study do not evidence the third rate process, since with these amines the third rate process has become faster than the second rate process. Consequently, only the rate-limiting second rate process is observed.

The fourth rate process (Figure 1D) evidenced in the reaction of oxaloacetic acid with primary and secondary amines is very slow and is subject to general-acid catalysis. This rate process is most likely attributable to decarboxylation through a cationic imine intermediate. In the case of primary amines, decarboxylation is subject to concerted general-acid catalysis (eq 16).

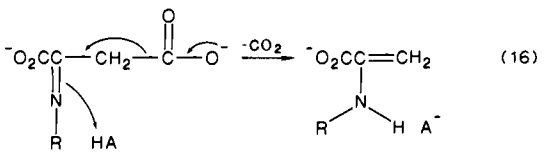

With secondary amines, the cationic imine intermediate is formed via rate-limiting general-acid-catalyzed protonation of the enamine, followed by rapid decarboxylation (eq 17). The sec-

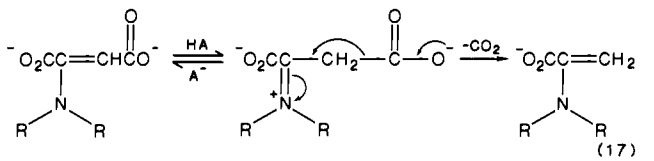

ond-order rate constants (k_{ga}''') for general acid catalyzed decarboxylation via the mechanisms of eq 16 and 17 are given in Table I; decarboxylation is a more facile process for the imine (eq 16) than for the enamine (eq 17), where the rate-limiting step is iminium ion formation. The logs of the intercepts of the buffer dilution plots for decarboxylation via eq 17 are plotted in Figure 10. The points refer to decarboxylation of five structurally dissimilar enamines; there appears to be little difference in the rates of water-catalyzed protonation, and there is a suggestion of specific-acid catalysis at low pH values.

It has long been known that the decarboxylation of β-keto acids such as acetonedicarboxylic acid and acetoacetic acid is catalyzed by primary amines.[11] The mechanism involves formation of an intermediate Schiff base which functions as an electron sink for the elimination reaction (eq 18), analogous to the mechanisms

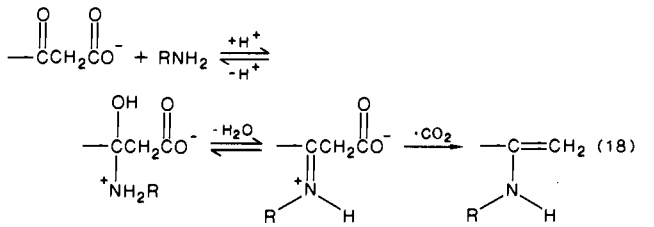

of Scheme I and eq 16 and 17. Secondary amines can also catalyze β-keto acid decarboxylation but, as was found in the present study, are not as effective as primary amines.[12] Enzymatic decarboxylation of acetoacetate takes place via intermediate Schiff base formation, as in eq 18, between the keto acid and a lysine residue of the enzyme.[13] Aspartate β-decarboxylase involves a similar mechanism (eq 19).[14]

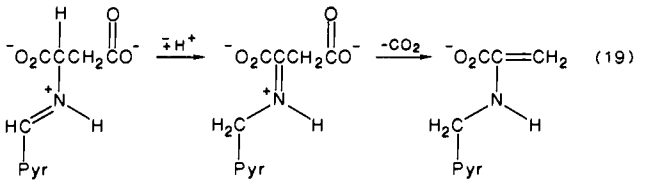

Acknowledgment. This research was supported by a grant from the National Institutes of Health to Thomas C. Bruice.

Registry No. Oxaloacetic acid, 328-42-7; ethylamine, 75-04-7; methylamine, 74-89-5; ethanolamine, 141-43-5; arginine, 74-79-3; tris, 77-86-1; glycine ethyl ester, 459-73-4; piperidine, 110-89-4; dimethylamine, 124-40-3; 2-(methylamino)ethanol, 109-83-1; ethyl *N*-piperazinecarboxylate, 120-43-4; 1-piperazinecarboxaldehyde, 7755-92-2; piperazine, 110-85-0.

(11) (a) Wiig, E. O. *J. Phys. Chem.* **1928**, *32*, 961. (b) Pedersen, K. J. *J. Am. Chem. Soc.* **1929**, *51*, 2098. (c) *Ibid.* **1938**, *60*, 595. (d) *J. Phys. Chem.* **1934**, *38*, 559. (e) Westheimer, F. H.; Jones, W. A. *J. Am. Chem. Soc.* **1941**, *63*, 3283.

(12) Hine, J.; Mulders, J. *J. Org. Chem.* **1967**, *32*, 2200.

(13) (a) Hamilton, G. A.; Westheimer, F. H. *J. Am. Chem. Soc.* **1959**, *81*, 6332. (b) Fridovich, I.; Westheimer, F. H. *J. Am. Chem. Soc.* **1962**, *84*, 3208. (c) Westheimer, F. H. *Proc. Chem. Soc. (London)* **1963**, 253. (d) Warren, S.; Zerner, B.; Westheimer, F. H. *Biochemistry* **1966**, *5*, 817. (e) Guthrie, J. P.; Westheimer, F. H. *Fed. Proc., Fed. Am. Soc. Exp. Biol.* **1967**, *26*, 562.

(14) (a) Nishimura, J. S.; Manning, J. M.; Meister, A. *Biochemistry* **1962**, *1*, 442. (b) Novogrodsky, A.; Nishimura, J. S.; Meister, A. *J. Biol. Chem.* **1963**, *238*, 1903. (c) Snell, E. E.; di Mari, S. J. *The Enzymes*; Academic: New York, 1970; Vol. 2, p 335. (d) Boeker, E. A.; Snell, E. E. *The Enzymes*; Academic: New York, 1972; Vol. 6, p 217.